Editors' Suggestion

Salt-induced Long-to-Short Range Orientational Transition in Water

Julien Duboisset[1,*] and Pierre-François Brevet[2]
[1]Aix Marseille Univ, CNRS, Centrale Marseille, Institut Fresnel, F-13013 Marseille, France
[2]Univ Lyon, Université Lyon1, Institut Lumière Matière, CNRS, UMR 5306, F-69622 Villeurbanne, France

(Received 12 January 2018; published 27 June 2018)

We report the long-range orientational organization of water using polarization-resolved second harmonic scattering operated in a right-angle configuration. A transition is observed between the neat water orientational organization involving an azimuthal molecular orientation distribution towards a radial molecular orientation distribution when salt is added. These two orientational phases are quantitatively described using a molecular model of the second harmonic scattering response. It is observed that the long-range correlation present in the neat water phase abruptly disappears and is replaced by a shorter range correlation centered around the ions as the salt concentration is increased.

DOI: 10.1103/PhysRevLett.120.263001

Liquid water continues to inspire great interest as its molecular organization and behavior is still not fully understood. Although it is well known that the short-range arrangement of water molecules is governed by steric hindrance, dipole interactions, and hydrogen bonds, long-range correlations are still considered to die out beyond few molecules distances [1]. Insights into short-range molecular distribution, orientation, and dynamics have been obtained using x rays [2–5], nuclear magnetic resonance [6], and optical measurements [7,8], as well as molecular dynamics simulations [9,10]. However, the counterintuitive picture where the liquid water molecules could be correlated over long distances is still not understood [11–15]. Here, we report that water molecules orientation at room temperature is correlated on distances that exceed several tens of nanometers, distances several orders of magnitude longer than expected. By performing polarization-resolved second harmonic scattering measurements on neat and salty water, we observe an orientational transition in the 1 mM salt concentration range. Water orientational organization switches from a several tens of nanometer organization to a radial distribution over several nanometers centered on the ions. Our results reveal the spatial structure of the water-water orientational organization and the characteristic correlation length. We establish the relationship between the correlation length and the salt concentration over 7 orders of magnitude. Hence, our quantitative observations call into question the currently accepted behavior of water and the way to describe water dynamics on large scales. Furthermore, we anticipate that such a behavior must be important in a number of biological and chemical problems, especially protein-water interaction or molecular transport.

Second harmonic scattering (SHS) is a nonlinear optical phenomenon involving the conversion of two photons at the fundamental frequency $\boldsymbol{\omega}$ into one photon at the harmonic frequency $2\boldsymbol{\omega}$ [16]. This second order process is forbidden, within the dipole approximation, in centrosymmetric media such as liquids. However, owing to the orientational fluctuations of the noncentrosymmetric water molecules, an incoherent intensity at the harmonic frequency is allowed, which corresponds to the sum of the intensity scattered by each single water molecule [16]. The SHS intensity I_{SHS} is formally given by

$$I_{\mathrm{SHS}} \propto \left\langle \left(\left\{ \hat{n} \times \left[\sum_i e^{i\varphi(\vec{r}_i'(t))} T(\vec{r}_i'(t)) \overleftrightarrow{\beta}_i \right] : \hat{e}\,\hat{e} \right\} \times \hat{n} \right) \times \left(\left\{ \hat{n} \times \left[\sum_i e^{i\varphi(\vec{r}_i'(t))} T(\vec{r}_i'(t)) \overleftrightarrow{\beta}_i \right] : \hat{e}\,\hat{e} \right\} \times \hat{n} \right)^* \right\rangle, \tag{1}$$

where $\hat{n} = \vec{r}/r$ is the unit vector of the collection direction, $\hat{e}$ is the unit vector of the electric field, and $\vec{r}_i'(t)$, $T(\vec{r}_i'(t))$, and $\overleftrightarrow{\beta}_i$ the position, the transformation tensor from the molecular to the laboratory frame, and the hyperpolarizability of molecule i. Also, $\varphi(\vec{r}_i'(t)) = K^{(2\omega)}|\vec{r} - \vec{r}_i'(t)| - 2\vec{k}^{(\omega)}\vec{r}_i'(t)$ is the phase vector, where $\vec{K}^{(2\omega)}$ and $\vec{k}^{(\omega)}$ are the scattered harmonic and the fundamental beam wave vectors, and the angular brackets $\langle ... \rangle$ stand for the time average. When molecule orientations are correlated, the scattered photons have well-defined phase differences. Because of the phase matching between these photons, the sensitivity to the correlation scales with r^2, meaning that the technique is magnifying the long-range correlations. At the difference of SHS, other techniques using femtosecond pulses (infrared pump-probe spectroscopy, for instance) are not sensitive to long correlations. This is because SHS requires noncentrosymmetric media and the signal recovered is sensitive to the deviation from the

centrosymmetry of the material, canceling the huge bulk contribution. Because of the use of optical wavelengths as opposed to short wavelengths normally used in say x-ray spectroscopy combined with an appropriate time average duration, SHS is an ideal tool to probe weak long-range correlations as observed in neat or salty water. Short wavelengths spectroscopy with long averaging time is on the opposite much better suited to investigate strong short-range correlations.

To investigate the orientational order of water molecules, the SHS signal is resolved in polarization. The measurements consist in acquiring the linearly polarized harmonic photons emitted at 90° with respect to the excitation, while the incoming beam linear polarization is rotated; see Fig. 1(a). The polarization signal follows the expression

$$I_{\mathrm{SHS}}(\alpha) = i_0 + i_2 \cos(2\alpha) + i_4 \cos(4(\alpha - \alpha_0)) \quad (2)$$

where i_0, i_2, and i_4 are the magnitude of the constant, the harmonic 2α and the harmonic 4α, respectively, and α_0 is the phase shift of the frequency 4α with respect to the frequency 2α. The parameters i_0 and i_2 are related to the water molecule first hyperpolarizability and i_4 to the long-range effects (see the equations in Supplemental Material [17]). These coefficients obey specific relationships depending on the nature of the emission. For a pure dipolar response, namely, for the case of randomly oriented molecules, the parameter i_4 coefficient vanishes [18]. On the contrary, if the correlation length is non-negligible in front of the optical wavelength, field retardation effects between correlated molecules break down the electric dipole approximation and i_4 differs from 0. In this context, a short-range or local correlation cannot explain the observed deviation from the electric dipole approximation [19]. To quantify the deviation from the case of a purely random liquid independently of the nonlinear cross section, the following normalized parameter is introduced,

$$I_4 = \frac{i_4 \cos 4\alpha_0}{i_0}, \quad (3)$$

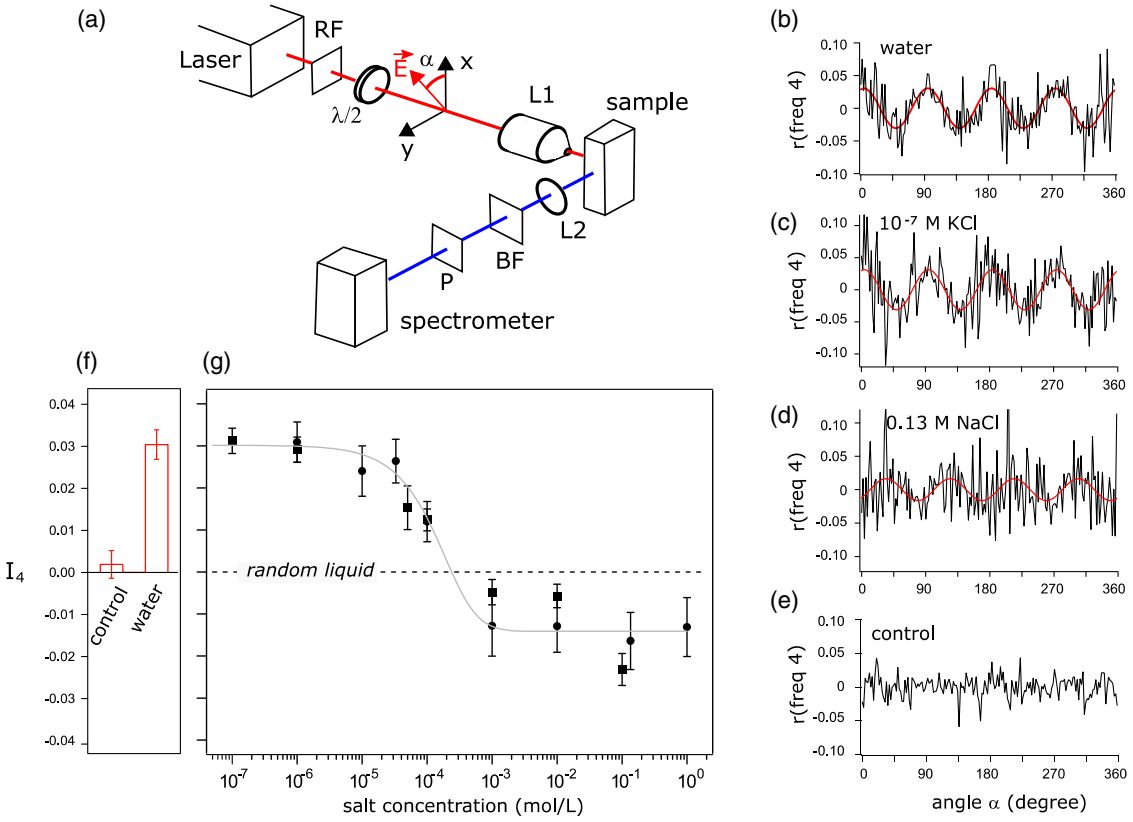

FIG. 1. Polarized second harmonic scattering experiments. (a) Experimental setup. A femtosecond laser beam is focused into a water cuvette through a red filter (RF), a half-wave plate, and a microscope objective (L1). The harmonic photon is detected at a right angle through a lens (L2), a blue filter (BF), and a vertical polarizer (P). The black line represents the residue of the signal at the frequency 4α, the red line corresponds to the fit for (b) neat water, (c) 10^{-7} M KCl, (d) 0.13 M NaCl, and (e) diluted molecule DiA in ethanol, where no correlations are expected. (f) Magnitude of I_4 for molecule DiA and water. (g) I_4 for different KCl (square) and NaCl (round) concentrations. I_4 is positive when the frequency 4α residue is positive at $\alpha = 0$ and negative when the frequency 4α residue is negative at $\alpha = 0$. The dashed line indicates $I_4 = 0$ corresponding to a pure random fluid. The gray line helps the reader. $\alpha = 0$ indicates that the laser beam is vertically polarized.

where I_4 is equal to 0 when the emission is purely dipolar, or different from 0 when retardation effects appear stemming from correlations between emitters.

From the polarimetric scans of $I_{\mathrm{SHS}}(\alpha)$ (see Supplemental Material Fig. S2 [17]), the constant intensity i_0 and the intensity i_2 at frequency 2α are subtracted in order to exhibit the residue only. For neat water, the residue of the polarimetric signal shows an oscillation at frequency 4α; see Fig. 1(b). Furthermore, one can note that the phase shift obeys $\alpha_0 = 0$, leading to a positive value of $I_4 = 0.03$. In order to prevent any experimental bias, the same measurements were performed on a control solution. This solution consisted of a high nonlinear cross section molecule [1 μM of DiA, 4-(4-dihexadecylaminostyryl)-*N*-methylpyridinium iodide] diluted in ethanol, where no correlation between DiA molecules is present due to the low concentration used [20]. As expected for a pure random distribution, the DiA residue does not show any signal at the harmonic 4α; see Fig. 1(e). For further investigations, NaCl and KCl salts were dissolved at various concentrations from 0.1 μM up to 1 M. It is indeed known that salts have the ability to disturb the neat water organization. At weak salt concentrations, the I_4 value is the same as that of neat water, showing that weak salt concentrations have no measurable effects, within the experiment sensitivity, on water behavior; see Fig. 1(c). However, a clear transition occurs in the range 0.01 M–1 mM. This range of concentrations typically corresponds to distances of about 20–40 nm between ions. After the transition, in the high concentration regime, the phase shift of the residue at frequency 4α changes to $\alpha_0 = \pi/4$, leading to a negative value of I_4; see Fig. 1(d). An orientational water structure transition is therefore observed as the salt concentration increases. At high concentrations, from mM to M, the I_4 values become significantly negative; see Fig. 1(g). Moreover, the I_4 value is almost constant in this mM to M concentration range. Two different salts where used to prevent any salt specificity. No significant change between the sodium and potassium cations was observed.

To interpret the significance of the I_4 value, we developed an analytical model of polarization-resolved SHS for different orientational organization of water. First, the microscopic components of the water first hyperpolarizability tensor were used [21]. Secondly, the resulting hyperpolarizability of the mesoscopic water structure was calculated by summing all the water molecule first hyperpolarizabilities, accounting for the different orientations and correlation length r; see Fig. 2(b). Thirdly, in order to determine the macroscopic hyperpolarizability involved in the SHS experiments, the mesoscopic first hyperpolarizability of these water structures is orientationnally averaged to take into account the isotropic nature of liquid water; see Fig. 2(c). We have investigated several generic geometries: (i) The random distribution where the orientation of molecules is random, (ii) the radial distribution where all water molecules point towards a unique center, (iii) the azimuthal distribution where water molecules are distributed along the φ angle, and (iv) the polar distribution where the water molecules are distributed along the θ angle. The resulting I_4 values are very different

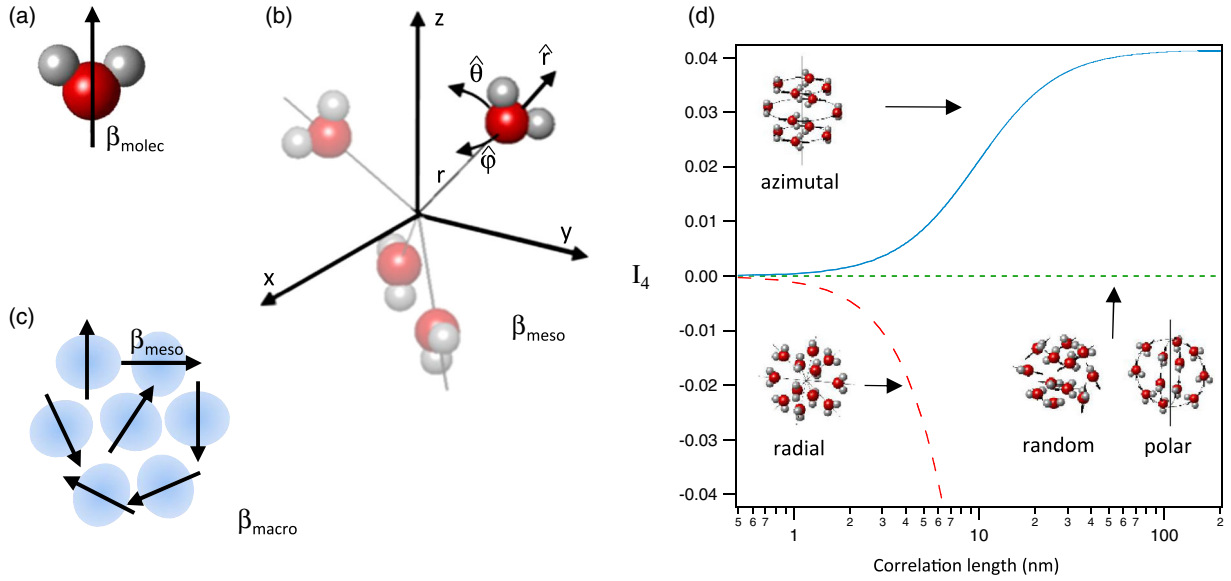

FIG. 2. Signal as a function of water structures and correlation length. From the water molecule hyperpolarizability (a), the mesoscopique hyperpolarizability is calculated by summing all the water molecule hyperpolarizabilities, accounting for the different orientations and correlation length r (b). Then the mesoscopic hyperpolarizability of these water structures is orientationally averaged in order to calculate the macroscopic hyperpolarizability (c) and I_4 (d). The different organizations show specific signatures. The azimuthal distribution (blue line) reaches a positive asymptotic value for long correlation length. Radial distribution (dashed red line) shows a quick decrease. Random and polar distribution (green dot line) do not have any contribution on I_4.

depending on the water orientational structure; see Fig. 2(d). For the random distribution, I_4 is equal to 0 due to the pure dipolar response without orientational correlation between molecules. For the radial distribution, I_4 is always negative and decreases rapidly with the correlation length r. For the azimuthal distribution, I_4 retains the asymptotic value of $I_4 = 0.03$. Finally, the polar distribution does not deviate from the random fluid behavior in the right angle scattering geometry and therefore I_4 is also equal to 0. The polar distribution is indeed noncentrosymmetric, but retardation effects incidentally play no role in this right-angle geometry, a case truly different from the radial and azimuthal distributions that are centrosymmetric [20].

The radial distribution is the only orientational structure in agreement with the negative values of I_4 observed at high salt concentrations. Such a value above 0 has already been observed for different molecular systems like spherical nanoparticles or micelles [19,20] and reveals a radial orientation of the correlated emitters. In the case of spherical micelles dispersed as aqueous suspensions, the amphiphilic molecules are radially oriented with their hydrophilic head pointing outside the micelles into the aqueous medium and the hydrophobic tail pointing inside the micelles [20]. Here, the average value determined is $I_4 = -0.04$ corresponding to a radial structure length of about 4 nm according to the model, meaning that molecules are pointing towards or away from the ions; see Fig. 2. This value is much longer than the radius of a few solvation shells observed by other techniques. However, the retardation effect contribution scales with r^2, giving a higher weight to the most distant molecules. The change in the sign of I_4 relates to the change in the geometry of the water organization in the 0.1 mM range. For neat water, the azimuthal distribution is the only structure providing positives values for I_4. Furthermore, the model, which does not possess any adjustable parameter, reaches the asymptotic value $I_4 = 0.03$ when the characteristic length of the orientational correlation structure reaches about 20 nm in length. This result bears out the transition in the 0.1 mM range, which corresponds to tens of nanometers between ions. This agreement suggests that the correlation length is in the 20 nm range for the neat water structure.

In order to attribute a characteristic length of the organization itself during the orientational transition, the correlation length r is plotted as a function of the salt concentration; see Fig. 3. For neat water and very small salts concentrations, long-range water molecules correlation structures are established. The maximum correlation length cannot be established accurately due to divergence of r with respect to I_4 in this regime; see Fig. 2(d). However, the minimum correlation length is above tens of nanometers. When the salt concentration increases, the correlation length decreases due to the presence of ions, which tends to disturb the correlation between water molecules. When the concentration reaches the 0.1 mM critical value, the water structure switches from

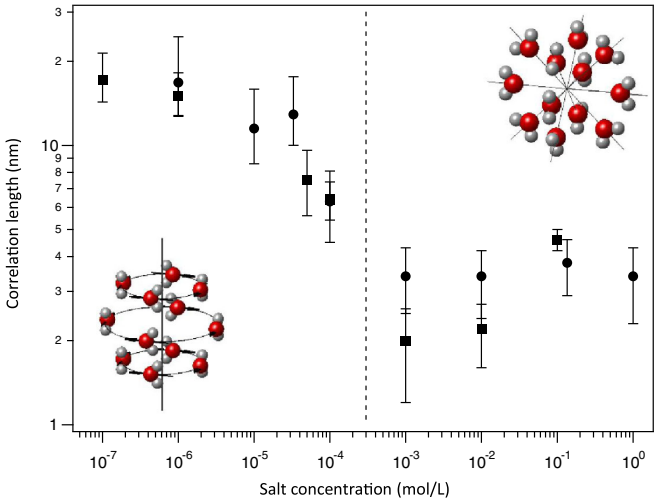

FIG. 3. Orientational correlation length as a function of salt concentration. In the high concentration regime, the radial distribution is established with a correlation length of 3 nm. When the concentration decreases, the distribution of water molecules switches to an azimuthal distribution and the correlation length increases up to several tens of nanometers. The radial and azimuthal models are used to attribute a correlation length. The maximum correlation length cannot be established accurately due to divergence of r with respect to I_4 in this regime; see Fig. 2. KCl (square) and NaCl (round). The dashed line helps the reader.

an azimuthal structure to a radial structure around the ions. The correlation length decreases down to about 3 nm and finally, at salt concentrations higher than 1 mM, the new orientational organization is fully established.

Whereas the radial organization can be well understood due to the dipolar moment that orients the molecules towards the ion direction, the correlation length is more unexpected. This fact is in contradiction with molecular dynamics studies [10] although recent experiments have observed long-range correlations [11,22,23] and theoretical work supports the ion influence over long distances [24]. In neat water, we quantify the correlation length to be at least 20 nm, a distance that far exceeds the classical distance obtained through others techniques. The nature of organization shows an azimuthal distribution of molecules, a behavior already observed in liquids that possess a strong dipole moment [25] and suspected for water but on a smaller scale [26,27].

In summary, we reveal the nature and the correlation of neat and salt water. In salt water, the polarization-resolved SHS experiments exhibit a correlation length of 3 nm and a radial structure of molecules. In neat water, we quantify the correlation length to be at least 20 nm with an azimuthal structure of molecules. Liquid water properties at the molecular level and the macroscopic level are rather well known today; however its properties at the nanoscale are not so well investigated, and therefore understood; whereas nonlinear optical measurements open access to long-range behavior.

Supplemental Material [17] is available in the online version of the paper.

The authors acknowledge financial support from the Agence Nationale de la Recherche ANR Tremplin-ERC (Grant No. ANR-16-TERC-0008-01) and ANR Racine (Grant No. ANR-2017-CE24-0029). J. D. conducted the experiments and developed the model. P.-F. B. conceived the study. J. D. and P.-F. B. wrote the manuscript. The authors declare no competing financial interests.

*Corresponding author.
julien.duboisset@fresnel.fr.

[1] J.-P. Hansen and J.-L. Barrat, *Basic Concepts for Simple and Complex Liquids* (Cambridge University Press, Cambridge, 2003).

[2] S. Bouazizi, F. Hammami, S. Nasr, and M.-C. Bellissent-Funel, Neutron scattering experiments on aqueous sodium chloride solutions and heavy water. Comparison to molecular dynamics and *x*-ray results, J. Mol. Struct. **892**, 47 2008.

[3] J. H. Guo, Y. Luo, A. Augustsson, J. E. Rubensson, C. Sathe, H. Agren, H. Siegbahn, and J. Nordgren, *X*-Ray Emission Spectroscopy of Hydrogen Bonding and Electronic Structure of Liquid Water, Phys. Rev. Lett. **89**, 137402 (2002).

[4] T. Takamuku, M. Tabata, A. Yamaguchi, J. Nishimoto, M. Kumamoto, H. Wakita, and T. Yamaguchi, Liquid structure of acetonitrile-water mixtures by *x*-ray diffraction and infrared spectroscopy, J. Phys. Chem. B **102**, 8880 (1998).

[5] S. Bouazizi, S. Nasr, N. Jaidane, and M.-C. Bellissent-Funel, Local order in aqueous NaCl solutions and pure water: *X*-ray scattering and molecular dynamics simulations study, J. Phys. Chem. B **110**, 23515 (2006).

[6] F. Mallamace, C. Corsaro, D. Mallamace, S. Vasi, and H. Stanley, NMR spectroscopy study of local correlations in water, J. Chem. Phys. **145**, 214503 (2016).

[7] A. Omta, M. Kropman, S. Woutersen, and H. Bakker, Negligible effect of ions on the hydrogen-bond structure in liquid water, Science **301**, 347 (2003).

[8] M. Cowan, B. Bruner, N. Huse, J. Dwyer, B. Chugh, E. Nibbering, T. Elsaesser, and R. Miller, Ultrafast memory loss and energy redistribution in the hydrogen bond network of liquid H2O, Nature (London) **434**, 199 (2005).

[9] T. A. Pham, C. Zhang, E. Schwegler, and G. Galli, Probing the electronic structure of liquid water with many-body perturbation theory, Phys. Rev. B **89**, 060202 (2014).

[10] G. Tocci, C. Liang, D. Wilkins, S. Roke, and M. Ceriotti, Second-harmonic scattering as a probe of structural correlations in liquids, J. Phys. Chem. Lett. **7**, 4311 (2016).

[11] Y. Chen, H. I. Okur, N. Gomopoulos, C. Macias-Romero, P. S. Cremer, P. B. Petersen, G. Tocci, D. M. Wilkins, C. Liang, M. Ceriotti, and S. Roke, Electrolytes induce long-range orientational order and free energy changes in the H-bond network of bulk water, Sci. Adv. **2**, e1501891 (2016).

[12] K. J. Tielrooij, N. Garcia-Araez, M. Bonn, and H. J. Bakker, Cooperativity in ion hydration, Science **328**, 1006 (2010).

[13] Y. Marcus, Effect of ions on the structure of water: Structure making and breaking, Chem. Rev. **109**, 1346 (2009).

[14] D. P. Shelton, Structural correlation in water probed by hyper-Rayleigh scattering, J. Chem. Phys. **147**, 154501 (2017).

[15] C. Zhang and G. Galli, Dipolar correlations in liquid water, J. Chem. Phys. **141**, 084504 (2014).

[16] K. Clays and A. Persoons, Hyper-Rayleigh Scattering in Solution, Phys. Rev. Lett. **66**, 2980 (1991).

[17] See Supplemental Material at http://link.aps.org/supplemental/10.1103/PhysRevLett.120.263001 for experimental method, data processing and SHS analytical model.

[18] S. Brasselet and J. Zyss, Multipolar molecules and multipolar fields: Probing and controlling the tensorial nature of nonlinear molecular media, J. Opt. Soc. Am. B **15**, 257 (1998).

[19] J. Nappa, I. Russier-Antoine, E. Benichou, C. Jonin, and P. Brevet, Second harmonic generation from small gold metallic particles: From the dipolar to the quadrupolar response, J. Chem. Phys. **125**, 184712 (2006).

[20] G. Revillod, J. Duboisset, I. Russier-Antoine, E. Benichou, G. Bachelier, C. Jonin, and P. Brevet, Multipolar contributions to the second harmonic response from mixed DiA-SDS molecular aggregates, J. Phys. Chem. C **112**, 2716 (2008).

[21] C. Liang, G. Tocci, M. D. Wilkins, A. Grisafi, S. Roke, and M. Ceriotti, Solvent fluctuations and nuclear quantum effects modulate the molecular hyperpolarizability of water, Phys. Rev. B **96**, 1041407 (2017).

[22] D. P. Shelton, Hyper-Rayleigh scattering from correlated molecules, J. Chem. Phys. **138**, 154502 (2013).

[23] C. Macias-Romero, I. Nahalka, H. I. Okur, and S. Roke, Optical imaging of surface chemistry and dynamics in confinement, Science **357**, 784 (2017).

[24] M. D. Wilkins, E. D. Manolopoulos, S. Rokke, and M. Ceriotti, Communications: Mean-field theory of water-water correlations in electrolytes solutions, J. Chem. Phys. **146**, 181103 (2017).

[25] D. P. Shelton, Are dipolar liquids ferroelectric? J. Chem. Phys. **123**, 084502 (2005).

[26] J. Higo, M. Sasai, H. Shirai, H. Nakamura, and T. Kugimiya, Large vortexlike structure of dipole field in computer models of liquid water and dipole-bridge between biomolecules, Proc. Natl. Acad. Sci. U.S.A. **98**, 5961 (2001).

[27] A. N. Dickey and M. J. Stevens, Site-dipole field and vortices in confined water, Phys. Rev. E **86**, 051601 (2012).